Development of a Sidescan Imagery Automated Roughness Estimation Algorithm

Marlin L. Gendron, Maura C. Lohrenz and Geary Layne
Naval Research Laboratory (NRL), Code 7440.1, Stennis Space Center, MS

ABSTRACT

An accurate estimation of seafloor roughness derived from sidescan imagery (SSI) is one of the components needed to determine bottom type of a geographic area for mine warfare. Analysts at the Naval Oceanographic Office (NAVOCEANO) historically have estimated roughness manually. This paper describes the development and testing of a prototype algorithm capable of deriving roughness from SSI. It also presents results from a feasibility study that showed that the algorithm correctly identified a smooth navigation lane and generated roughness polygons that are approximately 84% consistent with manual roughness polygons over the same area.

INTRODUCTION

The design and development of automated detection and classification algorithms is advancing rapidly in many fields, such as medicine. In 1967, Winsberg, et al. recognized the difficulty of viewing and analyzing large amounts of screening mammograms and suggested computer algorithms could help. There were also early attempts to identify lesions such as malignant tumors by using automated detection algorithms (Ackerman and Gose, 1972). Giger (2001) suggested automated algorithms should be considered for incorporation into all new medical digital imaging systems.

Estimations of bottom clutter and roughness are two of the components needed during Mine Warfare (MIW) operations to determine the seafloor type for a geographic area. Analysts at the Naval Oceanographic Office (NAVOCEANO) obtain bottom clutter and roughness estimations for MIW directly from sidescan sonar imagery (SSI). Detecting clutter and determining roughness manually can be time consuming and could produce inconsistent results. Automated algorithms can potentially derive clutter and roughness from SSI in a consistent and timely manner.

There are many different methods that aid in the extraction of features from SSI, including wavelet-denoising (Ioup et al., 2001) and neural networks (LeBlanc and Manolakos, 1991), but the software implementation of these methods often is not practical for real-time automated object detection in SSI. One extraction method commonly used is a technique that utilizes the Markov Random Field (MRF) model to segment the entire gray-scale SSI into bright regions ("brights"), dark regions ("shadows"), and reverberation (Murino, 2001; Reed et al., 2001; Reed et al., 2003). A bright corresponds to reflected acoustical energy, a shadow represents a lack of reflected energy, and what remains is so-called bottom reverberation (Mignotte et al., 2000).

In FY02, the Naval Research Laboratory (NRL) developed and delivered a real-time automated clutter detection and clustering algorithm to NAVOCEANO that was shown to identify regions of clutter in SSI quickly and in a repeatable manner. The automated clutter detection algorithm attempts to identify shadow and bright regions, as the SSI is being collected, and the clustering algorithm clusters the results at the end of a survey to derive clutter polygons. To obtain seafloor roughness polygons, NAVOCEANO analysts currently estimate the heights of seafloor objects by manually measuring the length of an object's acoustic shadow. This height information is manually clustered to determine the seafloor roughness polygons for an area. Because rocks, sand waves, and pock marks show up as shadows and bright spots in SSI, NRL's clutter detection algorithm could potentially be used to estimate seafloor roughness based on the heights of these objects via the length of their detected shadows.

In 2005, NAVOCEANO asked the authors to modify their clutter detection and clustering algorithm to utilize this height information to estimate seafloor roughness and automatically cluster the results. As part of a feasibility study to show whether or not a modified version of NRL's automated clutter detection algorithm could accurately estimate roughness, NAVOCEANO provided NRL with two data sets where roughness polygons were derived manually. NRL ran their modified clutter detection algorithm and clustered the results, which were then compared with the manually generated roughness polygons. This paper presents the results of this study.

1. REPORT DATE **MAR 2006**	2. REPORT TYPE		3. DATES COVERED **00-00-2006 to 00-00-2006**
4. TITLE AND SUBTITLE **Development of a Sidescan Imagery Automated Roughness Estimation Algorithm**			5a. CONTRACT NUMBER
			5b. GRANT NUMBER
			5c. PROGRAM ELEMENT NUMBER
6. AUTHOR(S)			5d. PROJECT NUMBER
			5e. TASK NUMBER
			5f. WORK UNIT NUMBER
7. PERFORMING ORGANIZATION NAME(S) AND ADDRESS(ES) **Naval Research Laboratory,Code 7440.1,1005 Balch Blvd,Stennis Space Center ,MS,39529**			8. PERFORMING ORGANIZATION REPORT NUMBER
9. SPONSORING/MONITORING AGENCY NAME(S) AND ADDRESS(ES)			10. SPONSOR/MONITOR'S ACRONYM(S)
			11. SPONSOR/MONITOR'S REPORT NUMBER(S)
12. DISTRIBUTION/AVAILABILITY STATEMENT **Approved for public release; distribution unlimited**			
13. SUPPLEMENTARY NOTES **Proceedings of the Industry Engineering and Management Systems (IEMS) 2006 Conference, 13-15 Mar, Cocoa Beach, FL**			
14. ABSTRACT **see report**			
15. SUBJECT TERMS			

16. SECURITY CLASSIFICATION OF:			17. LIMITATION OF ABSTRACT	18. NUMBER OF PAGES	19a. NAME OF RESPONSIBLE PERSON
a. REPORT **unclassified**	b. ABSTRACT **unclassified**	c. THIS PAGE **unclassified**	**Same as Report (SAR)**	**8**	

SIDESCAN SONAR IMAGERY (SSI)

A Sidescan Sonar System (SSS), deployed during the underwater survey of an area of interest, uses an acoustic transducer to send acoustical waves – or beams – through the water and receive them back to image the seafloor. The beams are sent in a wide angular pattern down to the bottom in swaths 100-500 meters wide, and the echoes are received back creating a narrow strip below and to the sides of the transducer track (Blondel and Murton, 1997). When SSS data is processed into SSI, image analysts can extract details about the local morphology of the seafloor.

The SSS can be hull-mounted, towed from a platform such as a ship or helicopter, or carried on-board an autonomous underwater vehicle (AUV). The SSS is usually equipped with pressure or altimeter sensors that allow it to follow the bottom, maintaining a constant height above the sea floor, or "fly" at a constant depth below the surface (Figure 1). To produce SSI, each scan line is sampled between 0 and 255 to produce intensity (grayscale) values. The imagery is built up one scan line of data at a time (Figure 2).
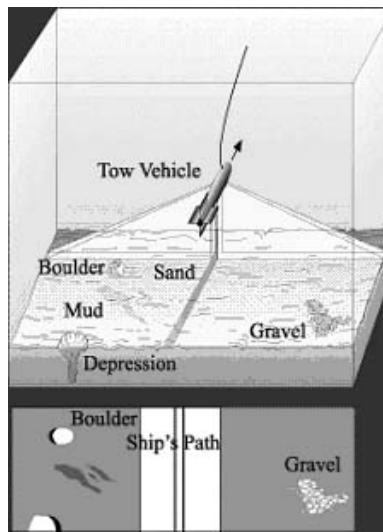

Figure 1. Illustration of a towed sidescan sonar system with resulting sidescan sonar imagery.
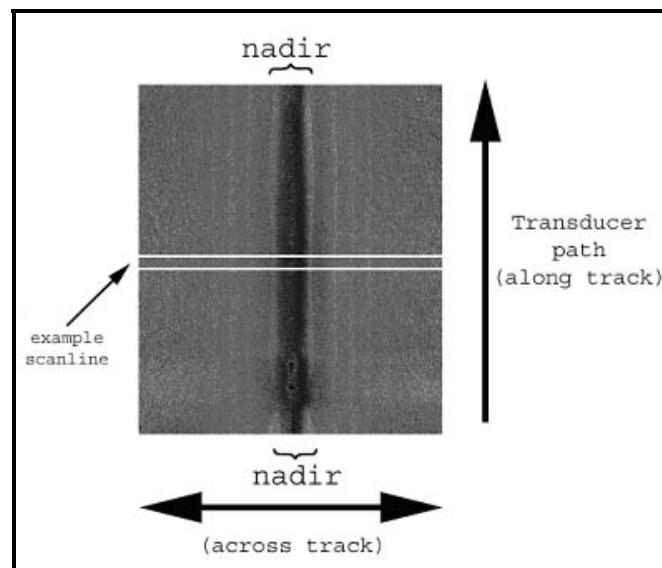

Figure 2.   Sidescan sonar imagery

The SSS data used in this paper was processed into imagery by NAVOCEANO and stored in the Unified Sonar Image Processing System (UNISIPS) format. Each scan line is stored in the UNISIPS file as a separate record. For any given line, the latitude and longitude coordinates at nadir, the position directly below the sonar, are known, as well as the heading of the sonar and its depth above the seafloor.

Features such as pockmarks, sand ripples, and rocks close to or on the seafloor are visible in the SSI. These objects are discernable as brights with adjacent shadows perpendicular to nadir. The dimensions of objects can be estimated as a function of the shadows' dimensions, but only the reflective structures of that portion of the object exposed above the seafloor can be estimated. These estimates are calculated along the object's two axes that are parallel and perpendicular to nadir. For example, the height of an object (above seafloor) can be estimated from the perpendicular dimension of the shadow (relative to nadir), which varies as a function of beam angle (Fish and Carr, 1990). Likewise, the length of the surface of the object facing the SSS can be estimated from the parallel dimension of the shadow. Figure 3 shows an example of a bottom object, or clutter, in SSI.
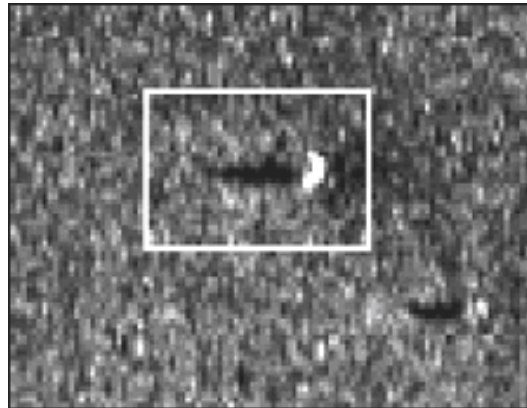
Figure 3. Bottom object detected in sidescan imagery

REAL-TIME AUTOMATED CLUTTER DETECTION ALGORITHM

The real-time automated detection algorithm developed by the authors ingests one UNISIPS scan line at a time. Across-track bright and shadow positions, lengths, and intensity information are immediately gathered from the scan line and stored in two one-dimensional geospatial bitmaps (GBs): one for shadows and one for brights.

Due to real-time processing considerations, the authors' algorithm relies on a GB technique (Gendron et al., 2001) patented by the author et al. Simple bitmaps – with a depth of one bit per pixel – are binary structures in which bits are turned on (set = 1) or off (cleared = 0). The index of each bit is unique and denotes its position relative to the other bits in the bitmap. The authors extended this concept to construct GBs in which every bit represents an object at some unique geospatial location. A set bit indicates that some object of interest exists (in this case a bright or shadow pixel) at that location, accurate to within the resolution of the bitmap. A cleared bit indicates the absence of any object at that location.

First, a modification to the common image processing technique called thresholding is used in the algorithm to extract shadows and brights from the scan line. Traditionally, thresholding is performed on an entire image, a process often called posterization, where select pixels, representing the foreground, are set to black and all other pixels (the background) are set to white to produce a binary image (Russ, 2002). The threshold is typically chosen in one of two ways: 1) ad hoc based on a histogram, or 2) interactively by a human after the entire image has been equalized (Russ, 2002). Because the authors' algorithm is automatic and operates in real-time, neither of these options is practical. Furthermore, two distinct thresholds are desired to capture both brights and shadows and all remaining pixels can be ignored.

Shadows and brights in a scan line are located by first adaptively obtaining a lower intensity bound, i_{min}, in which all samples of intensity lower than i_{min} are considered shadows. Likewise, an upper intensity bound, i_{max}, is found in which all samples of intensity that fall above i_{max} are considered brights. These intensity bounds are determined for each scan line, minus the center 10% of pixels, which are located close to nadir where the SSS is blind.

An appropriate gamma shift is used to convert the intensities of the image to fit a normal distribution, such that i_{min} and i_{max} could be set to the quartiles of the shifted (normal) distribution. Since the distribution of intensity values is different for each scan line, the gamma correction would also be different for each scan line. However, performing a gamma correction on every scan line to calculate intensity thresholds would be too computationally intensive to support a real time application. Therefore, the authors simply map the ideal i_{min} and i_{max} values from the standard normal distribution to the actual distribution via an approximation of the inverse gamma function, based on statistical measurements of each scan line's intensities

All pixels with intensity values above $I_{max}(x)$ are considered brights, while all with intensities below $I_{min}(x)$ are considered shadows, and the corresponding bits in the bright and shadow GBs are set (Figure 4).
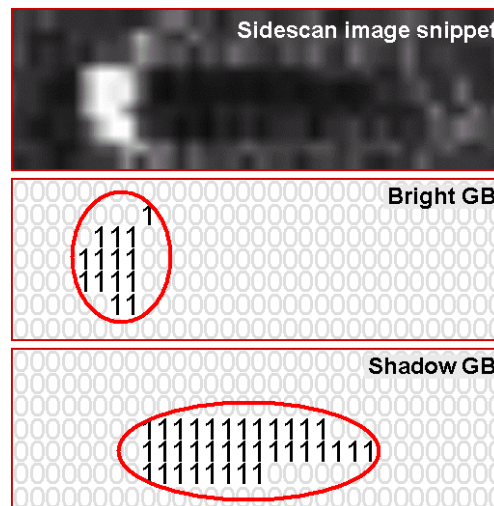

Figure 4. GBs facilitate clutter detection of objects in SSI. Each row of bits in both GBs corresponds to one scan line in the image. All pixels in the image with an intensity value greater than an upper threshold are considered "brights" and the appropriate bit in the bright GB is set. Likewise, all pixels in the image with an intensity value less than a lower threshold are considered "shadows" and the appropriate bit in the shadow GB is set.

The bright and shadow GBs are then examined from the outer edges of scan lines toward nadir to detect runs of shadows followed by runs of brights. (A valid object will have a shadow that falls away from nadir, with an adjacent bright closer to nadir). A circular lookup table is created to "window" the imagery several scan lines at a time. This lookup table is the same width as the GBs and is populated with the positions and run-lengths of shadows and brights stored in the GBs. The window information is then used to determine if there is an object present.

After the clutter detection algorithm is run on SSI from a survey area, the resulting latitude and longitude locations of objects are clustered by the authors' clustering algorithm to produce clutter polygons that show the bottom clutter density of the area.

**TESTING THE MODIFIED CLUTTER DETECTION ALGORITHM FOR ROUGHNESS**

In 2005, NAVOCEANO delivered two SSI imagery sets to the authors to test the ability of a modified clutter detection algorithm to estimate bottom roughness. Analysts at NAVOCEANO had already manually estimated the roughness of the two different geographic areas.

NRL modified their clutter detection algorithm such that height information from each detected bottom object was maintained. The height of a bottom object is estimated by measuring the length of its detected shadow. In the new roughness algorithm, the authors used the altitude of the SSS above the seafloor, the distance the shadow is from nadir, and the sonar resolution to compute, store, and cluster seafloor objects into polygons representing smooth and rough areas based on the heights of the objects.

Figure 5 shows smooth and rough polygons estimated manually by NAVOCEANO analysts for a large geographic area. NAVOCEANO provided SSI from "Test Box 1" and "Test Box 2", and the authors ran each data set through their new automated roughness algorithm. The algorithm was run on both test areas separately. The locations of objects detected by the algorithm for Test Box 1 were clustered and categorized into smooth and rough polygon. The left image in Figure 6 shows a mosaic of the SSI from Test Box 1 with the manual roughness polygons overlaid. The image on the right presents the results from the roughness and clustering algorithm. The "cluster radius", or the distance that two spatially close objects will be clustered, was adjusted in an attempt to create polygons of roughly the same size that the analyst drew.

Figure 7 shows the manual polygons overlaid on top of the results from the automated roughness algorithm. The percentage of agreement between the manual and automated polygons is approximately 53% and the percent correct, assuming the manual polygons to be ground truth, is 60%. Interestingly, both the manual and automated methods clearly indicate a smooth "lane" running through the center of the SSI. During MIW operations, bottom roughness is important because it is one of the components that is considered when choosing which navigation lanes to clear of mines. Typically, it is easier to clear a smooth seafloor than a rough one.

Figure 8 shows the manual and automated results from Test Box 2. Note that the manual roughness polygons (left, Figure 8) are larger than in Test Box 1 because the analyst chose to draw them larger, and the automated roughness polygons (right, Figure 8) are larger because a larger cluster radius was chosen during automated clustering. When overlaid, as shown in Figure 9, the percentage of agreement between the manual and automated polygons is approximately 64% and the percent correct is 84%. Note that the automated algorithm correctly preserved the smooth areas around the edges of the test area.
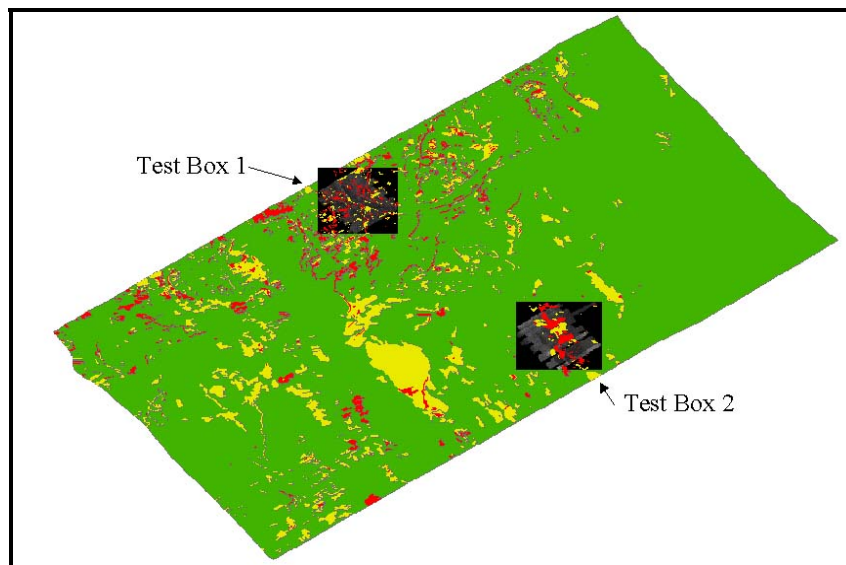
Figure 5. Test Boxes 1 and 2 provided to NRL to test their new roughness algorithm.
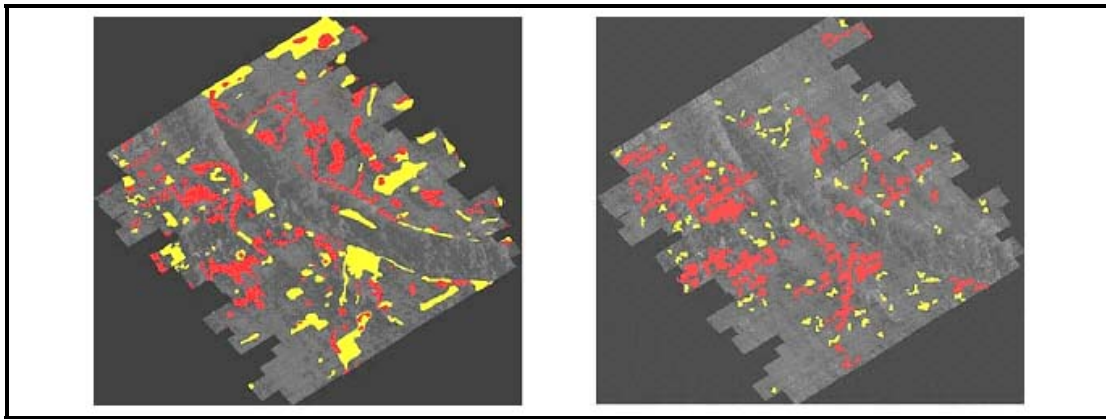
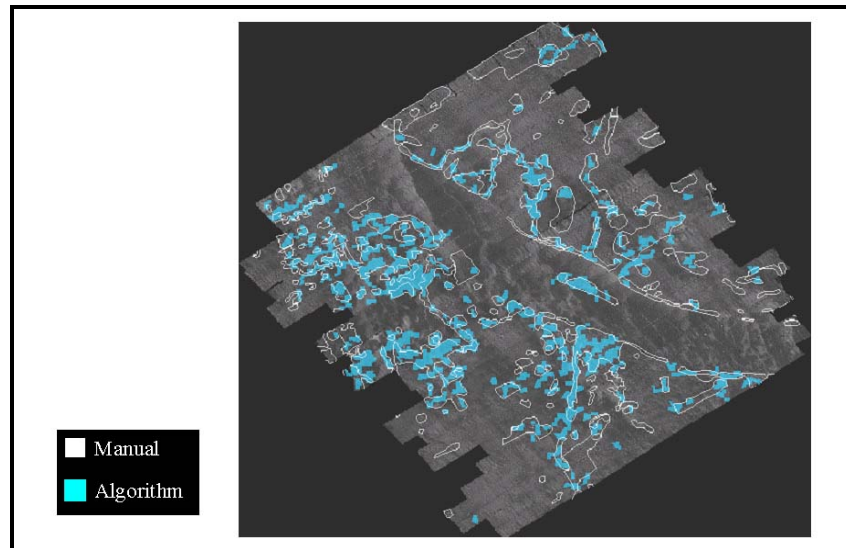*Figure 6. Manual (left) and Automated (right) roughness polygons for Test Box 1.*

Figure 7. Both the manual and automated roughness calculations indicate a smooth lane.
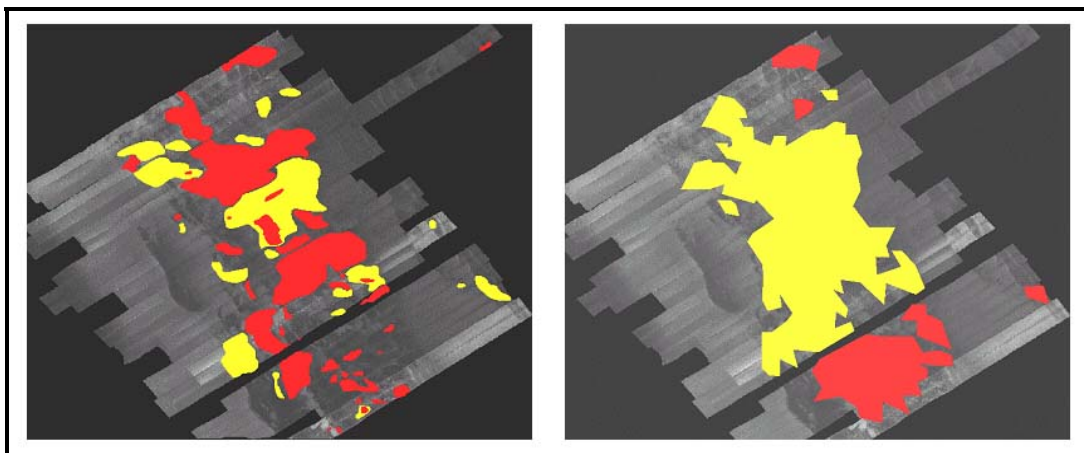

Figure 8. Manual (left) and Automated (right) roughness polygons for Test Box 2.

Figure 9. Manual roughness polygons overlaying automated roughness polygons for Test Box 2.

CONCLUSION

Estimating bottom roughness from SSI for a large survey area can take analysts months. This paper described a new roughness estimation algorithm that is capable of operating in real-time as imagery is being processed. The new algorithm presented was tested on two separate geographic areas where NAVOCEANO analysts have manually estimated bottom roughness. The automated roughness algorithm correctly identified a smooth lane in the first test area, and the generated automated roughness polygons were approximately 60% correct assuming the manual polygons to be ground truth. The algorithm correctly identified smooth areas around the edges of the second test area, and the generated automated roughness polygons were approximately 84% correct.

This feasibility study and modifications to the clutter detection algorithm for roughness estimation was accomplished over a few months in 2005. The results are promising, but do not yet reach the authors' target goal of 90% or greater correlation between automated and manual roughness polygons. The authors are currently studying the results of the feasibility study and have begun to make further modification to improve the new roughness algorithm.

ACKNOWLEDGEMENTS

REFERENCES

Ackerman, L.V. and E.E. Gose (1972). Breast Lesion Classification by Computer and Xeroradiograph. *Cancer*, October, 3:4.

Blondel, P. and B Murton (1997). *Handbook of Seafloor Sonar Imagery*. New York: John Wiley & Sons.

Fish, J. P. and Carr, H. A. Carr (1990). *Sound Underwater Images: A Guide to the Generation and Interpretation of Sonar*. American Underwater Search and Survey, Massachusetts: Lower Cape Publishing.

Gendron, M.L., P. B. Wischow, M.E. Trenchard, M.C. Lohrenz, L.M. Riedlinger, M. Mehaffey (2001). *Moving Map Composer*. Naval Research Laboratory, US Patent No. 6,218,965.

Giger, M.L. (2001). *CE: Mammography 4: Update on Computer-Aided Diagnosis in Mammography Handout*. AAPM meeting, Salt Lake City, Utah.

Ioup, Gendron, Bourgeois and Ioup (2001). Wavelet Denoising of Sidescan Sonar Images. Abstract of *the J. Acoust. Soc. Am.*, 110.

LeBlanc, M.J., E.S. Manolakos (1991). Neural Networks for Sidescan Sonar Automatic Target Detection. *Neural Networks for Signal Processing*, 1, Princeton, September.

Mignotte, M., C. Collet, P. Perez and P. Bouthemy (2000). Sonar Image Segmentation Using an Unsupervised Hierarchical MRF Model. *IEEE Transactions on Image Processing*, 9:7, July.

Murino, V. (2001). Reconstruction and Segmentation of Underwater Acoustic Images Combining Confidence Information in MRF Models. *Pattern Recognition*, 34:5.

Reed, S., Y. Petillot, J. Bell (2003). An Automatic Approach to the Detection and Extraction of Mine Features in Sidescan Sonar. *IEEE Journal of Oceanic Engineering*, 28:1, January.

Reed, S., Y. Petillot, and J. Bell (2001). Unsupervised Mine Detection and Analysis in Sidescan Sonar: A Comparison of Markov Random Fields and Statistical Snakes. Processings of *CAD/CAC 2001*, Halifax.

Russ, J. C. (2002). *The Image Processing Handbook, Fourth Ed. New York:* CRC Press.

Winsberg F., Elkin M., Macy J. et al. (1967). Detection of Radiographic Abnormalities in Mammograms by Means of Optical Scanning and Computer Analysis. *Radiology 1967*, 89.